

# Numerical Study on the flow field of a combustor with triple swirlers<sup>#</sup>

Chang Liu<sup>1</sup>, Peng Qian<sup>1</sup>, Zizhen Huang<sup>1</sup>, Zhiwei Chen<sup>1</sup>, Kai Han<sup>1</sup>, Jialei Zhang<sup>1</sup>, Wenjing Zhang<sup>1</sup>, Minghou Liu<sup>1\*</sup>

1 Department of Thermal Science and Energy Engineering, University of Science and Technology of China (USTC), Hefei, Anhui 230027, PR China

( \*Corresponding Author: mhliu@ustc.edu.cn )

## ABSTRACT

This paper conducts a numerical study on the characteristics of mean flow field of a combustor with triple swirlers with focus on the effect of turbulence models on the central recirculation zone (CRZ). By comparing numerical results with high-speed photography experiment, it is found that k- $\epsilon$  RNG model can better predict the flow field characteristics than k- $\epsilon$  realizable and k- $\omega$  SST model. The CRZ length and expansion angle obtained by k- $\epsilon$  RNG model are consistent with experiments, and k- $\epsilon$  Realizable model are relatively close to it, while k- $\omega$  SST model is quite different from the two others. The results predicted by k- $\omega$  SST have much higher backflow strength and pressure gradient. The study is of great significance to reasonably choice turbulent mode to predict swirling flow in a combustor.

**Keywords:** triple swirler; recirculation zone; turbulence model; Reynolds averaged Navier–Stokes

## NONMENCLATURE

### Abbreviations

CFD	computational fluid dynamics
CRZ	Central recirculation zone
RANS	Reynolds averaged Navier – Stokes modelling
LPM	lean premixed combustion

### Symbols

$Sn$	swirl number
$u$	axial velocity, m/s
$w$	tangential velocity, m/s
$k$	turbulent kinetic energy
$\epsilon$	dissipation rate
$\omega$	specific dissipation rate
$D$	swirler diameter

used lean premixed (LPM) combustion which reduce harmful emissions [1-2]. As its key component, the swirler plays an important role in achieving rapid fuel/air mixing and flame stabilization by utilizing vortex breakdown [3]. Swirlers can be classified into different kinds, such as single stage, double stage and triple stage, as well as axial and radial ones when classified by geometric arrangement [4]. At present, the research on single and double stage swirlers is relatively sufficient. Liu et al. [5] arranged two single-stage swirlers along the flow direction, and optimized the performance of the swirler through the combination of different vane angles; Liu et al. [6] carried out a numerical simulation to analyze the flow field of the dual-stage axial swirler combustion chamber, and found that the velocity distribution obtained by k- $\epsilon$  RNG model is more reasonable. However, due to the relatively complex geometric structure and the internal mechanism of triple swirlers, the related research is rarely reported. Vashahi et al. [7] changed the radial swirl number ( $Sn$ ) to explore the influence of vane length and passage width on the velocity distribution, and focused on the Coanda effect. In this paper, a triple swirler with two-stage axial and one-stage radial entrance is proposed for research with attention focused on the effect of turbulent model on the flow field of the combustor.

The usage of a swirler can create a low pressure central recirculation zone (CRZ) downstream, which is one of the most important features of flow field. It plays an important role in engineering applications such as fuel mixing and flame stabilization of combustion devices [8,9]. Tuttle et al. [10] described the importance of CRZ generation for the combustion process in the combustion chamber organization. Previous studies have shown that CRZ is related to swirls exceeding a certain swirl intensity [11]. The swirl intensity can be characterized by  $Sn$ , which is a dimensionless number that is defined as the ratio of axial flux of tangential to that of axial momentum. The expression is shown in Eq.(1), where  $R_i$  and  $R_o$  are the inner and outer radius, and  $u$  and  $w$  represent axial and tangential velocity

## 1. INTRODUCTION

Modern gas turbine spray combustors have attracted extensive research interest due to widely-

components, respectively. Regarding the effect of  $Sn$  on the distribution characteristics of

$$Sn = \frac{\int_{R_i}^{R_o} uwr^2 dr}{R_o \int_{R_i}^{R_o} u^2 r dr} \quad (1)$$

the flow field, Syred et al. [12] reviewed the effect of  $Sn$  on the length of the recirculation zone; Sanmiguel-Rojas et al. [13], and Beer et al. [15] studied the flow field characteristics of the recirculation zone with different  $Sn$  ranges. In addition to  $Sn$ , there are several other factors, including inlet conditions, geometry (such as vane angle [15]) and mass flow rate that affect the formation of the recirculation zone and the flame stability [16]. Knight et al. [17] concluded that the optimal design of the swirler should consider the mass flow rate at the inlet of combustion chamber. Stöhr et al. [18] obtained the results that changing the thermal power will change the structure of the flow field. Due to the complexity of the experiment and the difficulty in capturing the complex flow mechanism inside the flow field, computational fluid dynamics (CFD) methods have been widely used in recent years to predict the flow behavior and flow field characteristics [19]. However, different turbulence models were selected for simulation. Zavaleta-Luna et al. [20] proposed an optimal design for the swirler using k-ε RNG model, aiming to improve the working performance of the swirling flow field; Odabae et al. [21] confirmed that RANS simulation was consistent with experiments and saves computing time [22]. Agarwal et al. [23] used k-ε RNG model to study the effect of cone angle on the fluid velocity in the swirling field. Zianiet al. [24] chose three turbulence models namely k-ε model, modified k-ε model and RSM model for the study of the non-premixed combustion and compare the results with experiments. Selecting different turbulence models may have different degrees of influence on the results of various parameters of the flow field. Therefore, it is necessary to select an appropriate turbulence model in order to obtain better simulation results that are consistent with experiments.

The main objective of this study is to numerically simulate the cold flow field of a confined combustor with a triple swirler. Reynolds number is determined by controlling the inlet flow velocity, and the simulation results of the downstream flow field of the swirl combustion chamber are given. For validation, a high-speed photography experiment is conducted. The results have certain reference significance for selecting an appropriate turbulence model.

## 2. EXPERIMENTAL SETUP

Experiment is carried out in a combustion chamber to verify the simulation results. The schematic diagram of the experimental device is shown in Fig. 1. A laser sheet is used to illuminate the flow field in a certain section. The smoke produced by a smoke generator enters the combustion chamber from the entrance of the wind tunnel, and their motion trajectories are captured by a high-speed photography camera with a sampling frequency of 250 fps.

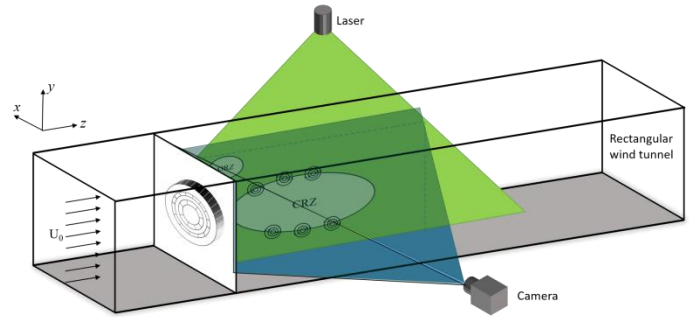


Fig. 1 schematic diagram of the experimental device

## 3. MESH INDEPENDENCE VERIFICATION AND DATA VALIDATION

In this paper, the three-dimensional steady-state RANS method is used to simulate the complex flow process of a combustion chamber with triple swirlers. The schematic diagram of the geometry is shown in Fig. 2. For different swirler entrances with swirl numbers of 0.46, 0.79, and 0.52 are investigated in this study to compare effects of turbulent model on the flow field inside gas turbine combustor. The working fluid is considered to be incompressible with constant thermal properties and the flow is assumed to be steady. For

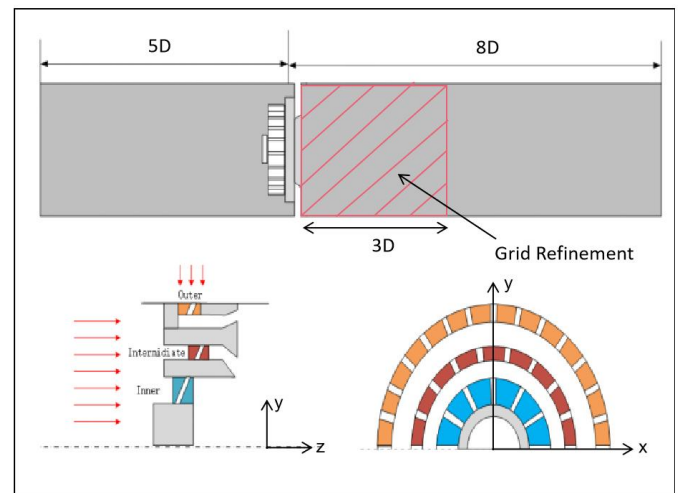


Fig. 2 schematic diagram of the combustor with triple swirlers

turbulent flow, the three-dimensional equations of continuity, momentum, turbulent kinetic energy  $k$  and the dissipation rate  $\varepsilon$  or specific dissipation rate  $\omega$  are solved. The governing equations are discretized using the windward difference scheme, and the SIMPLE algorithm is used to solve the discrete equations. The inlet and outlet boundary conditions are mass flow rate inlet and pressure outlet, respectively.

Due to the complex geometry of the triple swirlers, unstructured hexahedral meshes are used in this paper. In order to capture the recirculation zone downstream of the swirler outlet and fully develop the turbulent flow, the length of the inlet section is set to  $5D$  and the length of the outlet section is set to  $8D$ , and perform local grid refinement on the leading /trailing edges of the vane and the 3D area downstream the swirler outlet ( $D$  is the swirler diameter). The swirler outlet section is set at  $Z=0$ .

Air fluid density is  $1.185 \text{ kg/m}^3$ , and dynamic viscosity is  $1.835 \times 10^{-5} \text{ Pa} \cdot \text{s}$ . The Reynolds number is 6509. In order to effectively exclude the influence of grids on the simulation results, this paper selects three sets of grids (15.99 million, 7.69 million, and 4.83 million corresponding to mesh1, mesh2 and mesh3 respectively) for independent verification. The turbulence model used for verification is  $k-\varepsilon$  RNG.

Table 1 Grid independence verification

	Mesh1	Mesh2	Mesh3	Experiment
Length	1.75D	1.75D	1.85D	1.76D
Angle	$126.6^\circ$	$126.6^\circ$	$126.1^\circ$	$126.9^\circ$

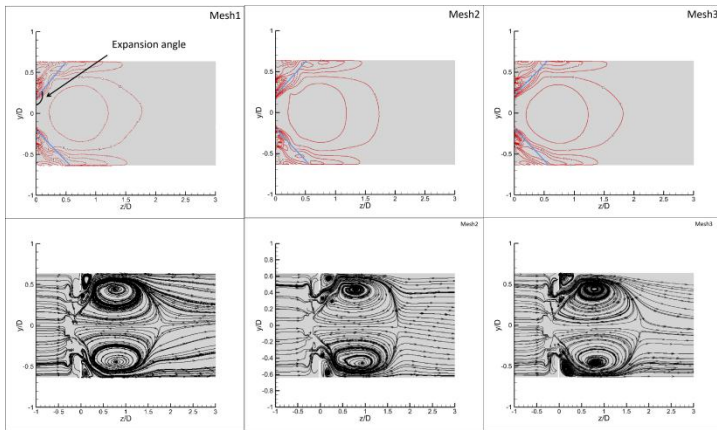


Fig. 3 expansion angle and streamlines at section  $x=0$

The swirl expansion angle and streamline distribution of the central section obtained by numerical simulation are shown in Fig. 3, and the experiment results under the same working condition is shown in

Fig. 4. The recirculation zone lengths and the expansion angles are compared in Table 1.

It can be seen that the results obtained by RANS simulation using the  $k-\varepsilon$  RNG turbulence model fit well with the experiment, the swirl expansion angles and the lengths of the recirculation zone are relatively consistent with the experiment results. The errors of the relevant characteristic parameters obtained by comparing the three sets of grids with the experimental results are all smaller than 6%. Therefore, mesh independence and numerical validity can be verified. In order to save the calculation cost and ensure the accuracy of the calculation results, this paper selects the grid Mesh2 for further research.

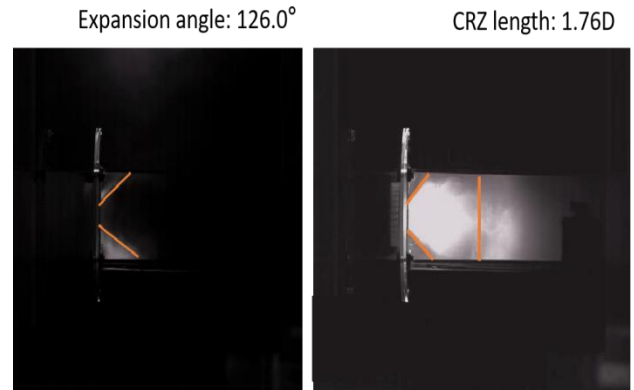


Fig. 4 experimental results of the expansion angle and the CRZ length

### 3. RESULTS AND DISCUSSION

In the previous part of this paper, the grid independence was verified, and the influence of the geometric model and the number of grids on the simulation results was preliminarily ruled out. Further, in order to compare the effects of different turbulence models to the flow field characteristics, three turbulence models, namely,  $k-\varepsilon$  RNG,  $k-\omega$  SST and  $k-\varepsilon$  Realizable, were selected for steady-state calculation. The inlet condition is the mass flow rate inlet with a magnitude of  $0.018 \text{ kg/s}$ ; the outlet condition is the pressure outlet. Menter-Lechner is selected as the wall function, which exhibits excellent convergence.

#### 3.1. Effect of the Turbulent Model on the Mean Velocity Field

In order to visually and clearly express the influence of different turbulence models on the CRZ, Fig. 5 shows the axial velocity contour and streamlines of  $x=0$  section. It can be seen that the velocity contours and streamline distribution of three turbulence models have good symmetry. Central recirculation zone and corner recirculation zone are both found in all three

models. However, the CRZ length varies, which are 0.65D, 1.75D, and 1.98D, respectively. Compared Fig. 5 with Fig. 4, it can be seen that RNG turbulence model is the most reasonable model, regarding CRZ length and expansion angle, while CRZ length obtained by k- $\epsilon$  Realizable is slightly longer, and is too shorter by k- $\omega$  SST.

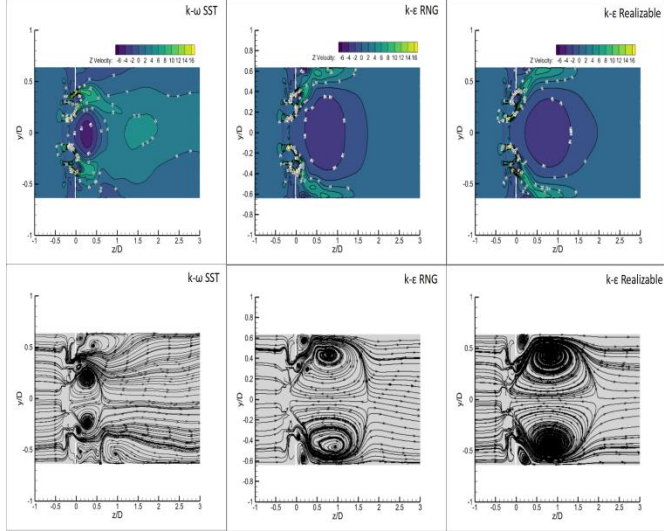


Fig. 5 velocity contours and streamlines corresponding to the three turbulence models. Left: k- $\omega$  SST; Middle: k- $\epsilon$  RNG; Right: k- $\epsilon$  Realizable

### 3.2. Effect of turbulence model on the radius and length of CRZ

Turbulence models may result in different CRZ radius and length. Fig.6 depicts the influence of turbulence model on CRZ length and radius. The results are summarized in Table 2.

Table 2 CRZ radius and length

	k- $\epsilon$ SST	k- $\epsilon$ RNG	k- $\epsilon$ Realizable
Radius	0.25D	0.49D	0.47D
Length	0.60D	1.75D	2.00D

The iso-surface of  $v_z=0$  is chosen to represent recirculation zones. Among three models, CRZ length and radius obtained by k- $\omega$  SST are the smallest. The results of k- $\epsilon$  RNG and k- $\epsilon$  Realizable are close. In addition, the volume of the recirculation zone corresponding to the k- $\epsilon$  RNG and k- $\epsilon$  Realizable turbulence models are  $12.5D^3$  and  $12.4D^3$ , respectively, which are almost the same, while the volume of the recirculation zone corresponding to the k- $\omega$  SST turbulence model is significantly smaller.

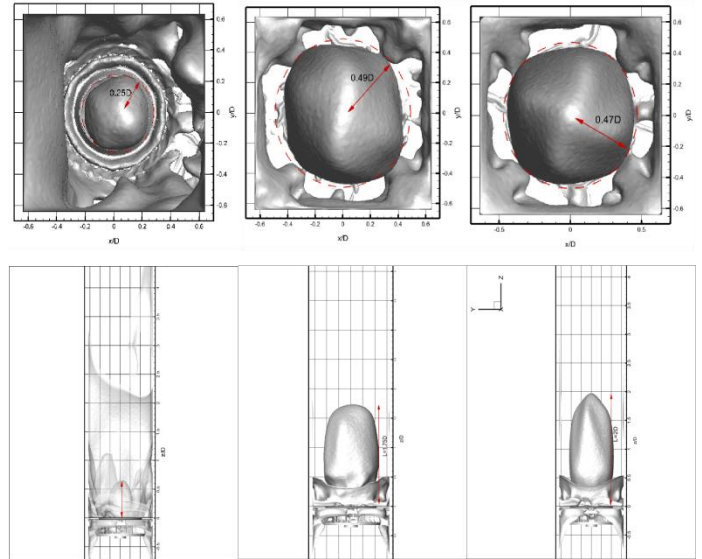
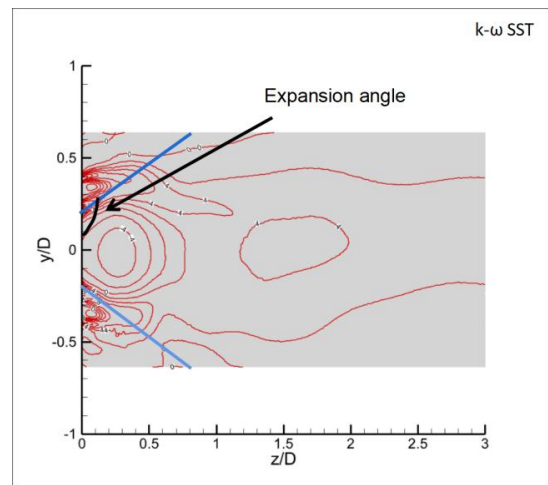


Fig. 6 CRZ Length and radius with different turbulence models

### 3.3. Effect of turbulence model on the characteristic parameters of CRZ

In order to clarify the influence of turbulence model on the characteristic parameters of CRZ, Fig. 7 shows the swirl expansion angle obtained by the numerical simulation corresponding to three turbulence models. The maximum flow expansion angle is obtained by k- $\epsilon$  Realizable model ( $128.62^\circ$ ), followed by k- $\epsilon$  RNG model ( $126.6^\circ$ ), and k- $\omega$  SST model ( $118.26^\circ$ ). Compared with experimental data shown in Fig. 4 ( $126.0^\circ$ ), the expansion angle obtained by k- $\epsilon$  Realizable and k- $\epsilon$  RNG are more reasonable, while k- $\omega$  SST model predicts a lower expansion angle.



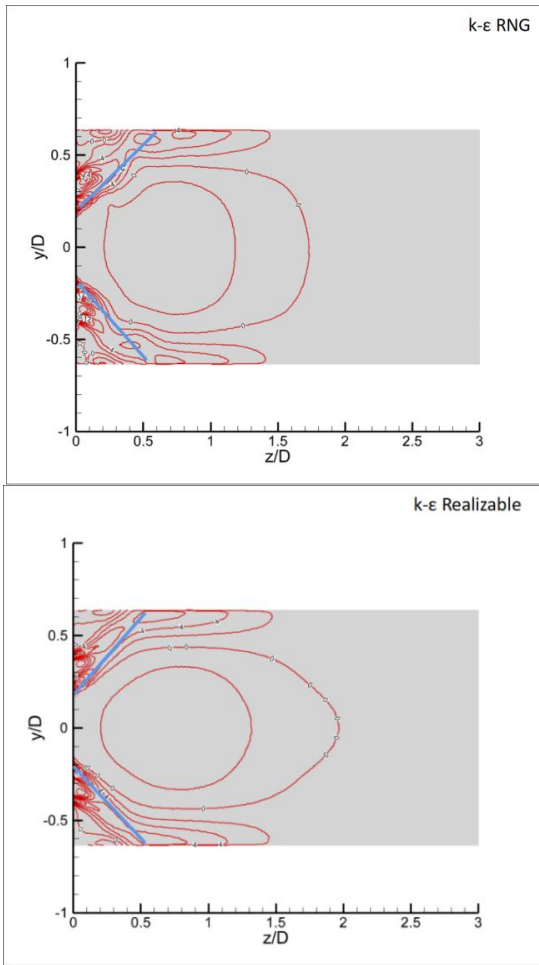


Fig. 7 expansion angle corresponding to different turbulence models

Fig. 8 shows vortex core position corresponding to three different turbulence models. It can be seen that all three models have relatively good symmetry. Among them, the vortex core position of k- $\omega$  SST model is the most symmetrical. Although the vortex core x-coordina-

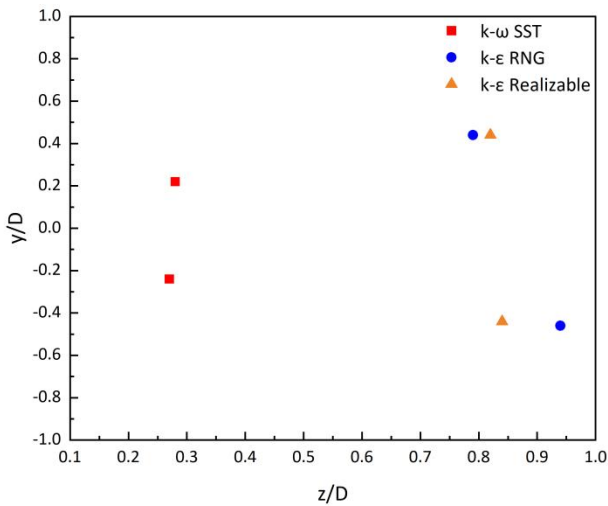


Fig. 8 the position of the vortex core corresponding to different turbulence models

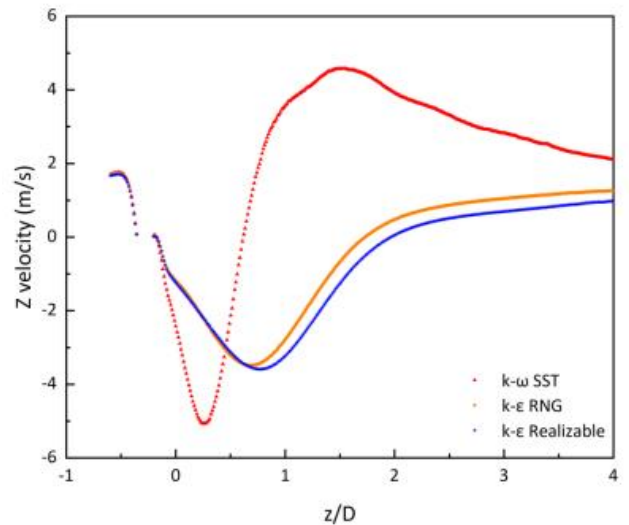
tes of k- $\epsilon$  models is different, the y-coordinates is nearly the same.

In order to explore the differences in the prediction results of different turbulence models for the velocity distribution, Fig. 9 shows axial velocity distribution and static pressure distribution corresponding to different turbulence models along centerline, and the results are shown in Table 3.

Table 3 maximum recirculation velocity and minimum pressure along centerline

	<i>k-<math>\omega</math> SST</i>	<i>k-<math>\epsilon</math> RNG</i>	<i>k-<math>\epsilon</math> Realizable</i>
Maximum			
recirculation	-5.07	-3.49	-3.59
velocity(m/s)			
Minimum			
Pressure(pa)	-27.84	-11.16	-10.74

It can be seen that the absolute value of the maximum recirculation velocity and the static pressure of the central axis corresponding to the k- $\omega$  SST model is larger than that of the other two models, and k- $\epsilon$  RNG and k- $\epsilon$  Realizable turbulence models are relatively close. In addition, the x-coordinates corresponding to the extreme points of the axial velocity and static pressure distribution corresponding to the k- $\omega$  SST model are much smaller than those of the other two models. The results predicted by k- $\omega$  SST have higher backflow strength and pressure gradient.



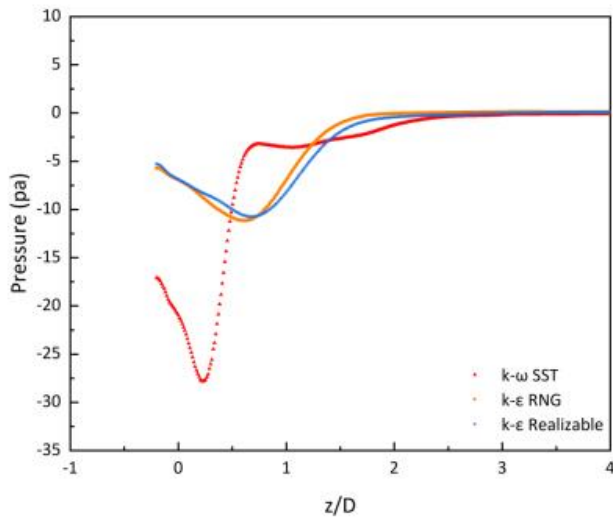


Fig. 9 axis velocity distribution and static pressure distribution corresponding to different turbulence models along centerline

#### 4 CONCLUSION

Central recirculation zone (CRZ) is one of the most important characteristics of the swirl field, and it has very important research significance. In this paper, the RANS numerical simulation method is used, and different turbulence models ( $k-\epsilon$  RNG,  $k-\omega$  SST and  $k-\epsilon$  Realizable) are applied to explore their influence on various characteristic parameters of CRZ. It provides a certain reference for selecting a suitable turbulence model for engineering applications. The following conclusions are drawn.

- 1) The prediction results for CRZ length and expansion angle obtained by  $k-\epsilon$  RNG model are consistent with experiments, and  $k-\epsilon$  Realizable model are relatively close to it, while  $k-\omega$  SST model is quite different from the two others.
- 2) The positions of the vortex cores corresponding to three turbulence models are generally symmetrical. The position of the vortex cores of  $k-\omega$  SST model is located upstream, which is much closer to the swirler outlet than the other two turbulence models.
- 3) Velocity and static pressure distribution corresponding to three turbulence models along centerline have similar trends, however,  $k-\omega$  SST model is different from the other two models: its maximum recirculation velocity is the largest and the minimum static pressure is smallest, while the other two models predicts close results.

#### REFERENCE

- [1] Revuelta, A. On the axisymmetric vortex breakdown of a swirling jet entering a sudden expansion pipe. *Physics of Fluids* 2004;16(9):3495–98.
- [2] Li, G. EMISSIONS, COMBUSTION DYNAMICS, AND CONTROL OF A MULTIPLE SWIRL COMBUSTOR[J]. *Emissions*, 2004.
- [3] G. C. Krieger, C. De, F. Sacomano. A swirler stabilized combustion chamber for a micro-gas turbine fuelled with natural gas. *Journal of the Brazilian Society of Mechanical Sciences & Engineering* 2012;34:441-49.
- [4] J. L. Halpin. Swirl Generation and Recirculation Using Radial Swirl Vanes. in *ASME 1993 International Gas Turbine and Aeroengine Congress and Exposition* 1993;3A: General.
- [5] L. Jing. Numerical analysis of the effect of swirl angle and fuel equivalence ratio on the methanol combustion characteristics in a swirl burner. *Process Safety and Environmental Protection* 2022;158:320-30.
- [6] Y. Zhang. Experimental and numerical investigations on flow field characteristics of pintle injector. *Aerospace Science and Technology* 2020; 103:105924.
- [7] F. Vashahi, S. Rezaei. Sensitivity analysis of the vane length and passage width for a radial type swirler employed in a triple swirler configuration. *Theoretical and Applied Mechanics Letters* 2019;9:363-75.
- [8] D. Durox et al. Flame dynamics of a variable swirl number system and instability control. *Combustion and Flame* 2013;160:1729-42.
- [9] P. Weigand, W. Meier. Investigations of swirl flames in a gas turbine model combustor. *Combustion and Flame* 2005;144:205-24.
- [10] Tuttle. Lean blowoff behavior of asymmetrically-fueled bluff body-stabilized flames. *Combustion and Flame* 2013;160:1677-1692.
- [11] N. Syred. A review of oscillation mechanisms and the role of the precessing vortex core (PVC) in swirl combustion systems. *Progress in Energy and Combustion Science* 2006;32:93-161.
- [12] N. Syred and J. M. Beér. Combustion in swirling flows: A review. *Combustion and Flame* 1974;23:143-201.
- [13] Sanmiguel-Rojas, E. Three-dimensional structure of confined swirling jets at moderately large Reynolds numbers. *Physics of Fluids* 2008; 20(4):044-104.
- [14] N. Syred and J. M. Beér. Combustion in swirling flows: A review. *Combustion and Flame* 1974;23:143-201.
- [15] A. K. Gupta. Swirl flows. *Combustion and Flame* 1984;63(1-2): 311.
- [16] Spalding, D. Combustion Aerodynamics. *Journal of Fluid Mechanics* 1972;54:762-762.

- [17] H. A. Knight. The Component Pressure Losses in Combustion Chambers. *Engineering, Environmental Science* 1957;16:617.
- [18] M. Sthr. Experimental study of vortex-flame interaction in a gas turbine model combustor. *Combustion and Flame* 2012;159:263649.
- [19] J.-F. Bourgooin, J. Moeck, D. Sensitivity of swirling flows to small changes in the swirler geometry. *Comptes Rendus Mécanique* 2013;341:211-19.
- [20] Zavaleta-Luna, D. Optimized Design of a Swirler for a Combustion Chamber of Non-Premixed Flame Using Genetic Algorithms. *Energies* 2020;13:2240.
- [21] M. Odabae, E. Sauret, and K. Hooman. ASME Turbo Expo 2016: Turbomachinery Technical Conference and Exposition. 2016.
- [22] F. Vashahi, J. Lee. On the emerging flow from a dual-axial counter-rotating swirler; LES simulation and spectral transition. *Applied Thermal Engineering* 2018; 129:646-56.
- [23] A. Agarwal, L. Mthembu. CFD analysis of conical diffuser under swirl flow inlet conditions using turbulence models. *Materials Today: Proceedings* 2020;27:1350-55.
- [24] L. Ziani, A. Numerical simulations of non-premixed turbulent combustion of CH<sub>4</sub> - H<sub>2</sub> mixtures using the PDF approach. *International Journal of Hydrogen Energy* 2013;38:8597-8603.